ARCHIVES of FOUNDRY ENGINEERING

ISSN (1897-3310)
Volume 10
Issue 4/2010

123 – 128

23/4

Published quarterly as the organ of the Foundry Commission of the Polish Academy of Sciences

Numerical analysis of short-pulse laser interactions with thin metal film

E. Majchrzak*, J. Poteralska
Department of Strength of Materials and Computational Mechanics
Silesian University of Technology
Konarskiego 18a, 44-100 Gliwice, Poland
*Corresponding author. E-mail address: ewa.majchrzak@polsl.pl

Received 30.06.2010; accepted in revised form 05.07.2010

Abstract

Thin metal film subjected to a short-pulse laser heating is considered. The hyperbolic two-temperature model describing the temporal and spatial evolution of the lattice and electrons temperatures is discussed. At the stage of numerical computations the finite difference method is used. In the final part of the paper the examples of computations are shown.

Keywords: Application of information technology to the foundry industry, Numerical techniques, Micro-scale heat transfer, Finite difference method

1. Introduction

The rapidly growing usage of femtosecond lasers in practical applications requires the description of very complex physical phenomena appearing in fast heating solids. The differences between the macroscopic model of heat conduction basing on the Fourier law and the models describing the ultrafast laser pulse interactions with metal films appear because of extremely short duration, extreme temperature gradients and geometrical features of domain considered.

Fast and highly nonequilibrium processes induced in the metals by the laser excitation can be described, among others, by two-temperature model (TTM) proposed by Anisimov et al. [1, 2, 3]. This model consists of two coupled differential equations

$$C_e(T_e)\frac{\partial T_e(x,t)}{\partial t} = -\nabla\cdot\mathbf{q}_e(x,t) - G\,[T_e(x,t) - T_l(x,t)] + Q(x,t)$$
$$C_l(T_l)\frac{\partial T_l(x,t)}{\partial t} = -\nabla\cdot\mathbf{q}_l(x,t) + G\,[T_e(x,t) - T_l(x,t)] \tag{1}$$

where T denotes temperature, $\mathbf{q}$ heat flux vector, $x=\{x_1, x_2, x_3\}$ are the spatial co-ordinates, t is the time, C is the heat capacity, λ thermal conductivity, G electron-lattice coupling factor, Q laser heating source, ∇ is the gradient operator. The quantities with superscripts e and l are associated with electrons and lattice, respectively.

In equations (1) the heat fluxes are defined as follows

$$\mathbf{q}_e(x,t) = -\lambda_e(T_e)\nabla T_e(x,t)$$
$$\mathbf{q}_l(x,t) = -\lambda_l(T_l)\nabla T_l(x,t) \tag{2}$$

and then the TTM consists of the system of parabolic equations.

Qiu and Tien [3, 4] derived a more general model in which the following dependencies between the heat fluxes and temperature gradients are introduced

$$\mathbf{q}_e(x,t+\tau_e) = -\lambda_e(T_e)\nabla T_e(x,t)$$
$$\mathbf{q}_l(x,t+\tau_l) = -\lambda_l(T_l)\nabla T_l(x,t) \tag{3}$$

where τ_e is the relaxation time of free electrons, this means the mean time for electrons to change their states in metals and τ_l is the relaxation time in phonon collisions.

Using the Taylor series expansions the following first-order approximation of equations (3) can be taken into account

$$\mathbf{q}_e(x,t)+\tau_e\frac{\partial \mathbf{q}_e(x,t)}{\partial t}=-\lambda_e(T_e)\nabla T_e(x,t)$$
$$\mathbf{q}_l(x,t)+\tau_l\frac{\partial \mathbf{q}_l(x,t)}{\partial t}=-\lambda_l(T_l)\nabla T_l(x,t) \quad (4)$$

The equations (1), (4) create the hyperbolic two-temperature model.

The following thermophysical properties appear in the two-temperature models: C_e, C_l, λ_e, λ_l, G and additionally in the hyperbolic TTM: τ_e, τ_l.

To define the thermal conductivity λ_e and heat capacity C_e of electrons the following relationships are widely used [2, 3]

$$\lambda_e(T_e,T_l)=\lambda_0\frac{T_e}{T_l}$$
$$C_e(T_e)=A_eT_e \quad (5)$$

where λ_0, A_e are the material constants. The remaining parameters, this means λ_l, C_l, G, τ_e, τ_l usually are assumed to be constant ones. It should be pointed out that the simple form of equation (5) is only suitable for temperatures T_e much smaller than Fermi temperature $T_F = E_F/k_B$, where E_F, k_B are the Fermi energy and Boltzmann constant, respectively [3].

2. Formulation of the problem

Let us consider a thin film of thickness L as shown in Figure 1. A front surface x=0 is irradiated by a laser pulse. Usually, the laser spot size is much larger than film thickness and then it is possible to treat the interactions as a one-dimensional (1D) heat transfer process [3].

The hyperbolic two-temperature model for 1D problem has the following form

$$C_e(T_e)\frac{\partial T_e(x,t)}{\partial t}=-\frac{\partial \mathbf{q}_e(x,t)}{\partial x}-G\,[T_e(x,t)-T_l(x,t)]+Q(x,t)$$
$$C_l(T_l)\frac{\partial T_l(x,t)}{\partial t}=-\frac{\partial \mathbf{q}_l(x,t)}{\partial x}+G\,[T_e(x,t)-T_l(x,t)] \quad (6)$$

where

$$\mathbf{q}_e(x,t)+\tau_e\frac{\partial \mathbf{q}_e(x,t)}{\partial t}=-\lambda_e(T_e)\frac{\partial T_e(x,t)}{\partial x}$$
$$\mathbf{q}_l(x,t)+\tau_l\frac{\partial \mathbf{q}_l(x,t)}{\partial t}=-\lambda_l(T_l)\frac{\partial T_l(x,t)}{\partial x} \quad (7)$$

Mathematical formula determining the intensity of internal heat source $Q(x, t)$ resulting from laser action can be assumed in the following form

$$Q(x,t)=\sqrt{\frac{\beta}{\pi}}\frac{1-R}{t_p\,\delta}I_0\exp\left[-\frac{x}{\delta}-\beta\frac{(t-2t_p)^2}{t_p^2}\right] \quad (8)$$

where I_0 is the laser intensity, t_p is the characteristic time of laser pulse, δ is the optical penetration depth, R is the reflectivity of the irradiated surface and $\beta = 4\ln 2$ [3].

The local and temporary value of $Q(x, t)$ results from the distance x between surface subjected to laser action and the point considered.

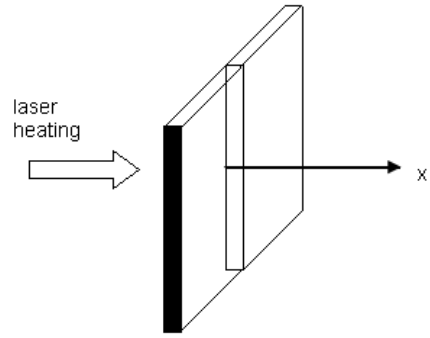

Fig. 1. Thin film

Taking into account the short period of laser heating, heat losses from front and back surfaces of thin film can be neglected [3], this means

$$q_e(0,t)=q_e(L,t)=q_l(0,t)=q_l(L,t)=0 \quad (9)$$

where $q_e(x, t)$, $q_l(x, t)$ are the heat fluxes for electron and lattice systems, respectively.

The initial conditions are assumed to be constant

$$t=0:\ T_e(x,0)=T_l(x,0)=T_p \quad (10)$$

3. Method of solution

To solve the problem formulated the finite difference method [5, 6, 7] is adapted. A staggered grid is introduced [8, 9] (Figure 2). Let us denote $T_i^f=T(ih, f\Delta t)$, where h is a mesh size, Δt is a time step, $i=0, 2, 4, ..., N$, $f=0, 1, 2, ..., F$, and $q_j^f=q(jh, f\Delta t)$, where $j=1, 3, ..., N$-1.

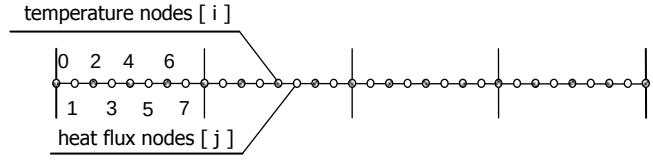

Fig. 2. Discretization

The finite difference approximation of equations (7) using explicit scheme can be written in the form

$$\mathbf{q}_{ej}^{f-1}+\tau_e\frac{\mathbf{q}_{ej}^{f}-\mathbf{q}_{ej}^{f-1}}{\Delta t}=-\lambda_{ej}^{f-1}\frac{T_{ej+1}^{f-1}-T_{ej-1}^{f-1}}{2h} \quad (11)$$

and

$$\mathbf{q}_{j}^{f-1}+\tau_l\frac{\mathbf{q}_{lj}^{f}-\mathbf{q}_{j}^{f-1}}{\Delta t}=-\lambda_{j}^{f-1}\frac{T_{lj+1}^{f-1}-T_{lj-1}^{f-1}}{2h} \quad (12)$$

where index j corresponds to the 'heat flux nodes' (Figure 2).

Equations (11), (12) can be transformed as follows

$$q_{ej}^{f}=\frac{\tau_e-\Delta t}{\tau_e}q_{ej}^{f-1}-\frac{\lambda_{ej}^{f-1}\Delta t}{2h\tau_e}(T_{ej+1}^{f-1}-T_{ej-1}^{f-1}) \quad (13)$$

and

$$q_{lj}^{f}=\frac{\tau_l-\Delta t}{\tau_l}q_{lj}^{f-1}-\frac{\lambda_j^{f-1}\Delta t}{2h\tau_l}(T_{lj+1}^{f-1}-T_{lj-1}^{f-1}) \tag{14}$$

The dependencies (13), (14) allow one to construct the similar formulas for nodes i-1, i+1 and then one obtains

$$q_{ei-1}^{f}-q_{ei+1}^{f}=\frac{\tau_e-\Delta t}{\tau_e}\ q_{ei-1}^{f-1}-q_{ei+1}^{f-1}\ +$$
$$\frac{\Delta t}{2h\tau_e}\left[\lambda_{ei-1}^{f-1}(T_{ei-2}^{f-1}-T_{ei}^{f-1})+\lambda_{ei+1}^{f-1}(T_{ei+2}^{f-1}-T_{ei}^{f-1})\right] \tag{15}$$

and

$$q_{li-1}^{f}-q_{li+1}^{f}=\frac{\tau_l-\Delta t}{\tau_l}\ q_{li-1}^{f-1}-q_{li+1}^{f-1}\ +$$
$$\frac{\Delta t}{2h\tau_l}\left[\lambda_{li-1}^{f-1}(T_{li-2}^{f-1}-T_{li}^{f-1})+\lambda_{li+1}^{f-1}(T_{li+2}^{f-1}-T_{li}^{f-1})\right] \tag{16}$$

Now, we discretize equations (6) using the explicit scheme of finite difference method

$$C_{ei}^{f-1}\frac{T_{ei}^{f}-T_{ei}^{f-1}}{\Delta t}=-\frac{q_{ei+1}^{f}-q_{ei-1}^{f}}{2h}-G\left[T_{ei}^{f-1}-T_{li}^{f-1}\right]+Q_i^{f-1} \tag{17}$$

and

$$C_{li}^{f-1}\frac{T_{li}^{f}-T_{li}^{f-1}}{\Delta t}=-\frac{q_{li+1}^{f}-q_{li-1}^{f}}{2h}+G\left[T_{ei}^{f-1}-T_{li}^{f-1}\right] \tag{18}$$

where index i corresponds to the 'temperature nodes' as shown in Figure 2.

Putting (15) into (17) and (16) into (18) one has

$$C_{ei}^{f-1}\frac{T_{ei}^{f}-T_{ei}^{f-1}}{\Delta t}=\frac{(\tau_e-\Delta t)}{2h\tau_e}(q_{ei-1}^{f-1}-q_{ei+1}^{f-1})+$$
$$\frac{\Delta t}{4h^2\tau_e}\left[\lambda_{ei-1}^{f-1}(T_{ei-2}^{f-1}-T_{ei}^{f-1})+\lambda_{ei+1}^{f-1}(T_{ei+2}^{f-1}-T_{ei}^{f-1})\right]-$$
$$G\left[T_{ei}^{f-1}-T_{li}^{f-1}\right]+Q_i^{f-1} \tag{19}$$

and

$$C_{li}^{f-1}\frac{T_{li}^{f}-T_{li}^{f-1}}{\Delta t}=\frac{(\tau_l-\Delta t)}{2h\tau_l}(q_{li-1}^{f-1}-q_{li+1}^{f-1})+$$
$$\frac{\Delta t}{4h^2\tau_l}\left[\lambda_{li-1}^{f-1}(T_{li-2}^{f-1}-T_{li}^{f-1})+\lambda_{li+1}^{f-1}(T_{li+2}^{f-1}-T_{li}^{f-1})\right]+$$
$$G\left[T_{ei}^{f-1}-T_{li}^{f-1}\right] \tag{20}$$

From equation (19) results that

$$T_{ei}^{f}=\left(1-A_{ei}^{f-1}-B_{ei}^{f-1}-\frac{G\Delta t}{C_{ei}^{f-1}}\right)T_{ei}^{f-1}+A_{ei}^{f-1}T_{ei-2}^{f-1}+$$
$$B_{ei}^{f-1}T_{ei+2}^{f-1}+\frac{G\Delta t}{C_{ei}^{f-1}}T_{li}^{f-1}+\frac{\Delta t(\tau_e-\Delta t)}{2h\tau_e C_{ei}^{f-1}}\ q_{ei-1}^{f-1}-q_{ei+1}^{f-1}\ +\frac{Q_i^{f-1}\Delta t}{C_{ei}^{f-1}} \tag{21}$$

where:

$$A_{ei}^{f-1}=\frac{(\Delta t)^2\lambda_{ei-1}^{f-1}}{4h^2\tau_e C_{ei}^{f-1}},\quad B_{ei}^{f-1}=\frac{(\Delta t)^2\lambda_{ei+1}^{f-1}}{4h^2\tau_e C_{ei}^{f-1}} \tag{22}$$

From equation (20) results that

$$T_{li}^{f}=\left(1-A_{li}^{f-1}-B_{li}^{f-1}-\frac{G\Delta t}{C_{li}^{f-1}}\right)T_{li}^{f-1}+A_{li}^{f-1}T_{li-2}^{f-1}+$$
$$B_{li}^{f-1}T_{li+2}^{f-1}+\frac{G\Delta t}{C_{li}^{f-1}}T_{ei}^{f-1}+\frac{\Delta t(\tau_l-\Delta t)}{2h\tau_l C_{li}^{f-1}}\ q_{li-1}^{f-1}-q_{li+1}^{f-1} \tag{23}$$

where

$$A_{li}^{f-1}=\frac{(\Delta t)^2\lambda_{li-1}^{f-1}}{4h^2\tau_l C_{li}^{f-1}},\quad B_{li}^{f-1}=\frac{(\Delta t)^2\lambda_{li+1}^{f-1}}{4h^2\tau_l C_{li}^{f-1}} \tag{24}$$

In numerical computations the following approximation of thermal conductivities has been used (c.f. equations (22), (24))

$$\lambda_{ei-1}^{f-1}=\frac{\lambda_{ei}^{f-1}+\lambda_{ei-2}^{f-1}}{2},\quad \lambda_{ei+1}^{f-1}=\frac{\lambda_{ei}^{f-1}+\lambda_{ei+2}^{f-1}}{2} \tag{25}$$

$$\lambda_{li-1}^{f-1}=\frac{\lambda_{li}^{f-1}+\lambda_{li-2}^{f-1}}{2},\quad \lambda_{li+1}^{f-1}=\frac{\lambda_{li}^{f-1}+\lambda_{li+2}^{f-1}}{2} \tag{26}$$

and (c.f. equations (12), (13))

$$\lambda_{ej}^{f-1}=\frac{\lambda_{ej-1}^{f-1}+\lambda_{ej+1}^{f-1}}{2},\quad \lambda_{lj}^{f-1}=\frac{\lambda_{lj-1}^{f-1}+\lambda_{lj+1}^{f-1}}{2} \tag{27}$$

Summing up, for transition $t^{f-1}\rightarrow t^{f}$ at first the equations (13), (14) should be solved and next using the equations (21), (23) the temperatures T_e and T_l are determined.

It should be pointed out that adequate stability criteria for explicit scheme must be fulfilled, this means (equations (13), (14))

$$\frac{\tau_e-\Delta t}{2h\tau_e}\geq 0$$
$$\frac{\tau_l-\Delta t}{2h\tau_l}\geq 0 \tag{28}$$

and (c.f. equations (21), (23))

$$\left(1-A_{ei}^{f-1}-B_{ei}^{f-1}-\frac{G\Delta t}{C_{ei}^{f-1}}\right)\geq 0$$
$$\left(1-A_{li}^{f-1}-B_{li}^{f-1}-\frac{G\Delta t}{C_{li}^{f-1}}\right)\geq 0 \tag{29}$$

4. Examples of computations

The values of thermophysical parameters of selected metals are collected in the Table 1. At the stage of numerical computations it is assumed that the lattice thermal conductivity equals to $\lambda_l=\lambda_0$, electron thermal conductivity is proportional to T_e/T_l, this means $\lambda_e=\lambda_0 T_e/T_l$ and electrons volumetric specific heat is proportional to the electrons temperature $C_e=A_eT_e$ (c.f. equation (5)). The remaining parameters are assumed to be constant. Additionally, in the table 1 the melting temperature T_m for each metal is placed.

The film of thickness L=100 nm (1nm =10^{-9} m) is considered. Initial temperature equals T_p =300 . The layer is subjected to a short-pulse laser irradiation (R =0.93, I_0 =10 J/m^2, t_p =0.1 ps, δ=15.3 nm).

The problem is solved using finite difference method under the assumption that Δt =0.001 ps and h =1 nm.

In Figures 3, 4, 5 and 6 the calculated electrons and lattice temperature profiles in Au and Cu thin films are shown. Figure 7 illustrates the heating (cooling) curves T_e, T_l at the front surface (x =0) for Au and Cu, respectively

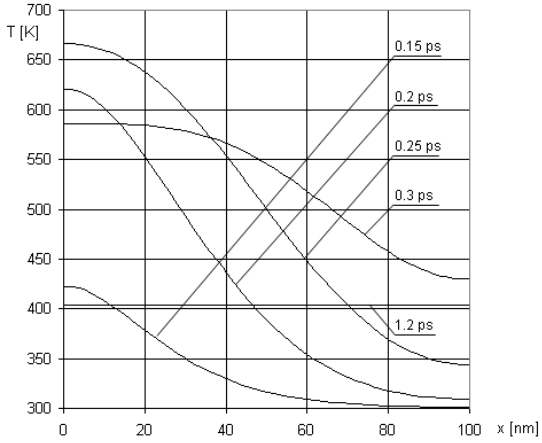

Fig. 3. Electron temperature profiles for Au

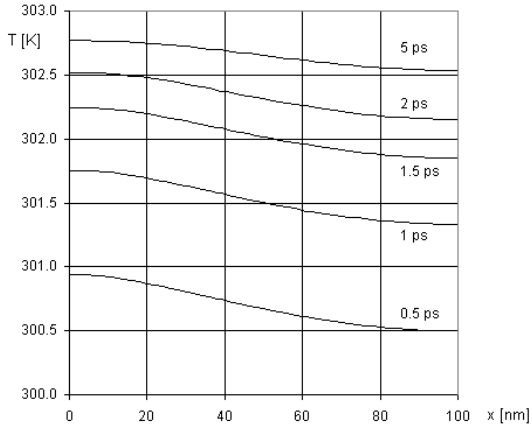

Fig. 4. Lattice temperature profiles for Au

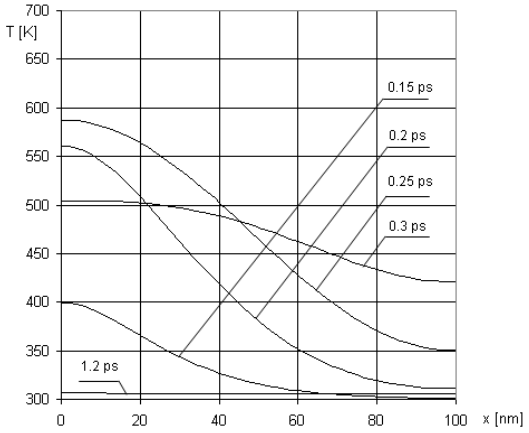

Fig. 5. Electron temperature profiles for Cu

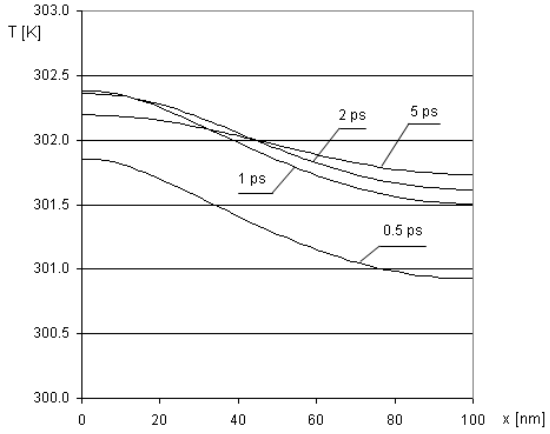

Fig. 6. Lattice temperature profiles for Cu

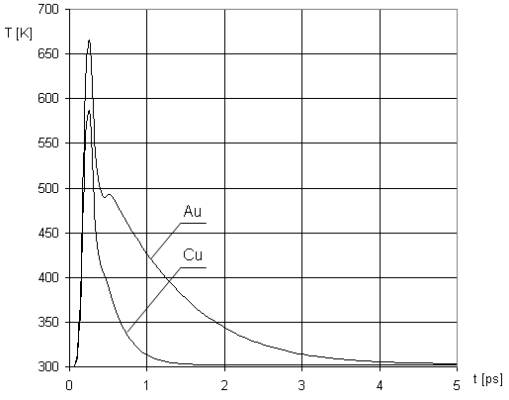

Fig. 7. Time history of the electrons temperatures at the front surface (x = 0) for Au and Cu

Table 1.
Thermophysical parameters for selected metals [2, 10]

	Ag	Cu	Au	W	Ti
λ_0 [W/(mK)]	429	409	315	173	21.9
A_e [J/(m^{3}K^2)]	62.8	71.0	62.9	137.3	328.9
C_l [J/(m^{3}K)]	$2.62 \cdot 10^6$	$3.39 \cdot 10^6$	$2.5 \cdot 10^6$	$3 \cdot 10^6$	$2.34 \cdot 10^6$
G [W/(m^{3}K)]	$3.5 \cdot 10^{16}$	10^{17}	$2.6 \cdot 10^{16}$	$5 \cdot 10^{17}$	$1.3 \cdot 10^{18}$
τ_e [ps]	0.04	0.03	0.04	0.01	0.01
τ_l [ps]	0.6	0.6	0.8	0.2	0.5
T_m [K]	1235	1358	1337	3695	1941

It is visible, that the results are different for these materials. Although the Cu thermal conductivity λ_0 is greater than Au thermal conductivity, both the electrons and the lattice temperatures in Cu film are lower in comparison with Au film. This results from the differences in values of coupling factor between these materials - the coupling factor for Cu is essentially greater than for Au.

It should be pointed out that for Au thin film the temperatures obtained agree very well with experimental results presented in [3].

Similar computations have been done for others materials. As an example, Figures 8-10 illustrate the temperature distributions for Ti and W.

It should be pointed out that the results presented here allow, among others, to determine the thermalization time corresponding to the equalization of electrons and lattice temperatures (c.f Figures 10 and 13). After the thermal equilibrium between electrons and the lattice occurs, the calculations can be done using one macroscopic hyperbolic equation [3].

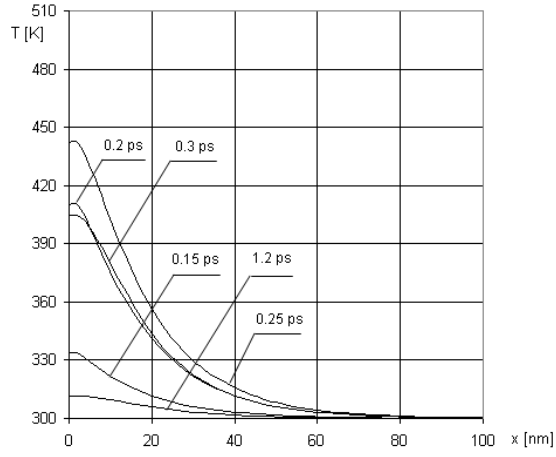

Fig. 8. Electron temperature profiles for Ti

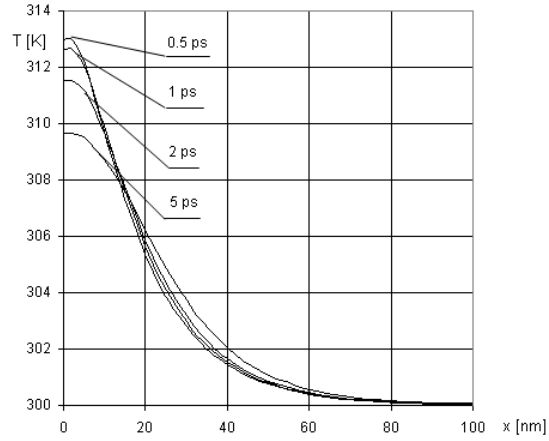

Fig. 9. Lattice temperature profiles for Ti

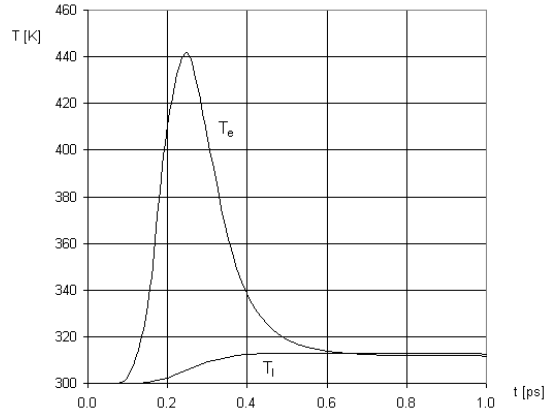

Fig. 10. Time history of the electron and lattice temperatures at the front surface (x = 0) for Ti

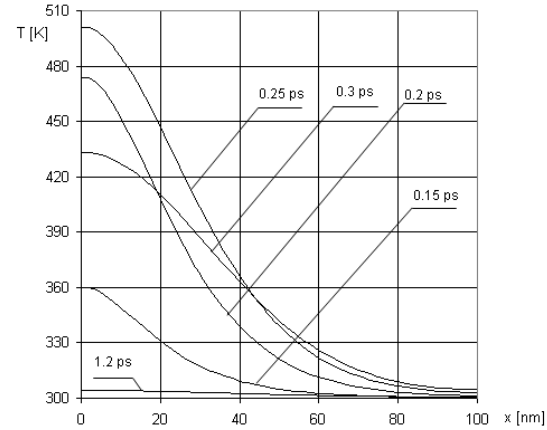

Fig. 11. Electron temperature profiles for W

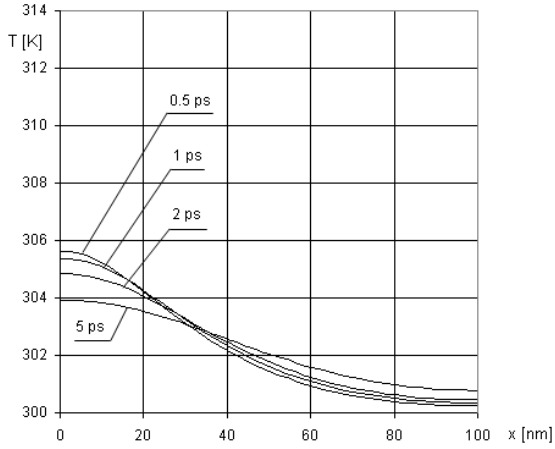

Fig. 12. Lattice temperature profiles for W

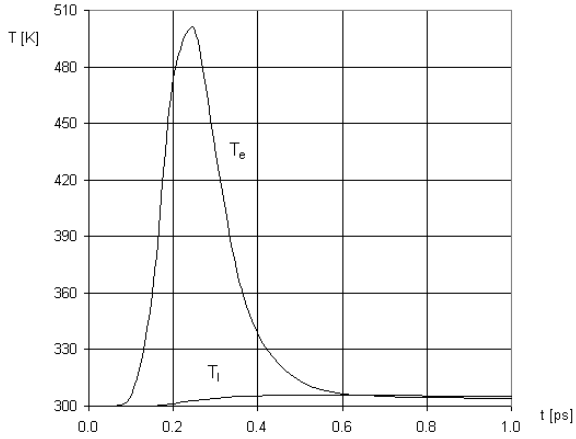

Fig. 13. Time history of the electron and lattice temperatures at the front surface ($x = 0$) for W

5. Conclusions

The problems discussed in this paper concern only the heating process proceeding in metal films subjected to the strong external heat flux, the phase changes (e.g. melting or ablation) are not taken into account. From the mathematical and numerical points of view the generalization of the task discussed here on the more complex thermal problems is not very complicated. The main difficulty is the proper choice of thermophysical parameters of material for the high temperatures and the formulation of the model determining the phase changes in domain for which the heat transfer processes proceed according to the hyperbolic two-temperature model. The investigations in this range are at present realized.

Acknowledgement

This work was funded by Grant No N N501 2167 37.

References

[1] S.I.Anisimov, B.L.Kapeliovich, T.L.Perel'man, Electron emmision from metal surfaces exposed to ultrashort laser pulses, Sov. Phys. JETP, vol. 39, 1974, pp. 375-377.

[2] Z.Lin, L.V.Zhigilei, Electron-phonon coupling and electron heat capacity of metals unde conditions of strong electron-phonon nonequilibrium, Physical Review, B 77, 2008, pp. 075133-1-075133-17.

[3] J.K.Chen, J.E.Beraun, Numerical study of ultrashort laser pulse interactions with metal films, Numerical Heat Transfer, Part A, 40, 2001, pp. 1-20.

[4] T.Q.Qiu, C.L.Tien, Femtosecond laser heating of multi-layer metals - I Analysis, Int. J. Heat Mass Transfer, vol. 37, 1994, pp. 2789-2797.

[5] B.Mochnacki, E.Pawlak, Identification of boundary condition on the contact surface of continuous casting mould, Archives of Foundry Engineering, Vol. 7, 4, 2007, 202-206.

[6] B.Mochnacki, J.S.Suchy, Numerical methods in computations of foundry processes, Polish Foundrymen's Technical Association, Cracow, 1995.

[7] E.Majchrzak, J.Mendakiewicz, Application of FDM for numerical solution of hyperbolic heat conduction equation, Scientific Research of the Institute of Mathematics and Computational Science, Czestochowa, 1(5), 2006, 134-139.

[8] W.Dai, R.Nassar, A compact finite difference scheme for solving a one-dimensional heat transport equation at the microscale, J. of Comput. and Applied Mathematics, 132, 2001, pp. 431-441.

[9] E.Majchrzak, J.Poteralska, Numerical modelling of short-pulse laser interactions with thin metal films using two-temperature model, 18th Int. Conf. on Computer Methods in Mechanics, CMM 2009, 2009, Zielona Góra, Short Papers, 295-296.

[10] E.Kannattey-Asibu Jr., Principles of laser materials processing, John Wiley & Sons, Inc., Hoboken, New Yersey, 2009.